

Multichannel Color Spaces Selection for Region-Based Active Contour: Applied to Plants Extraction Under Field Conditions

Yamina Boutiche(✉), Nabil Chetih, Naim Ramou, Mohammed Khorchef, and Rabah Abdelkader

Research Center in Industrial Technologies - CRTI, ex CSC, P.O.Box 64, Cheraga, 16014 Algiers, Algeria
y.boutiche@crti.dz
https://www.crti.dz

Abstract. Segmentation in agriculture presents a challenging issue especially when acquisition conditions are not controlled. Segmentation algorithms should be able to deal with images that can contain shadowed regions, upper/less lighted parts and saturated pixels. Consequently, the segmentation of RGB images is more often failed. In this paper, we propose a method that can overcome some of the listed difficulties. It is based, firstly, on a transformation of RGB color space into $L^*a^*b^*$, HSV and YC_rC_b ones. Secondly, to benefit from chroma information only, a^*, H and C_b are selected and combined to construct the image to be segmented. Finally, the Piecewise Constant (PC) Chan-Vese model with fast optimization principle is adopted for the segmentation issue.

Experiments are carried out in plant images with controlled conditions and field conditions using four open datasets. In addition, an evaluation study is done using three different metrics. The obtained results show the effectiveness and the robustness of the proposed approach compared to single-channel (color index-based) approaches and the multi-channel based segmentation.

Keywords: Agricultural images · Segmentation · Plant extraction · PC active contours · Fast sweep optimization

1 Introduction

The use of image processing and analysis in agriculture is experiencing remarkable growth, where a large image processing techniques have been exploited for several issues. Automatic segmentation of plants [1–3], leaf extraction [4], leaf disease detection [5,6], irrigation control [10], fruit recognition and counting [7].

The challenging tasks in agriculture are providing algorithms and color analysis techniques that should be able to deal with the non-trivial and uncontrollable capture conditions such as shadows, noise, pixel saturation, low lighting present the real difficulties for the image processing community.

© Springer Nature Switzerland AG 2021
O. Gervasi et al. (Eds.): ICCSA 2021, LNCS 12950, pp. 163–173, 2021.
https://doi.org/10.1007/978-3-030-86960-1_12

Almost all acquisition systems provide images defined on RGB color space, where each pixel is initially represented in the three components Red, Green and Blue. The RGB color space and its derived obtained by a linear transformations are generally not suitable for color scene segmentation and analysis because of the high correlation between their three components [8]. In fact, there is non same opinion about the color space that provides the best performance in color image segmentation issue. Therefore, for each specific application, researchers try to find an optimum color space where an algorithm gives a high segmentation accuracy. Several studies have been carried out to evaluate algorithms of color images segmentation. For example, in [9] comparison studies between different color spaces in clustering-based image segmentation was carried on general nature images.

In the context of agricultural images segmentation, Hamuda et *al.* have done a survey and an evaluation of plant extraction based on color indices [20]. In [10] authors presented a comparisons between color models for automatic image analysis in irrigation management applications. A review on weed detection using ground-based machine vision and image processing techniques was done in [11].

In this paper, we propose a chroma combination between the three color spaces $L^*a^*b^*$, HSV and YC_rC_b. This purpose allows to benefit from color space transformation advantages, especially in term of the separation between chroma and luminance information. Then, instead of using all color space components, we select one chroma component of the above spaces which are a^*, H and C_b. Those components are combined to construct three-components image. The segmentation step is done by the Piecewise-Constant Chan-Vese model optimized by sweeping algorithm for fast convergence.

The paper is organized as follows: Sect. 2 details the stages of the proposed method. Experiments results and comparisons are given in Sect. 3. Finally, the main conclusions are done in Sect. 4.

2 Proposed Method

The present work is devoted to segment agricultural images, where they are acquisition in an uncontrolled light conditions. Figure 1 represents the flowchart of the proposed method. We develop each stage in the following subsections.

2.1 Color Space Transformations

Color spaces can be grouped into four main groups *Primary spaces*, *luminance-chrominance spaces*, *perceptual spaces* and *independent axis spaces* [12].

The great advantage of the three last groups is their ability to separate between luminance and chroma information. However, there are different opinions about the transformation that allows the best segmentation performance. Nevertheless, some comparative studies have been done in [13] and [10]. In [10] a comparative study of eleven color spaces for the problem of plant segmentation is described. The best ones were found to be HLS, HSV, YC_rC_b, YUV, $L^*a^*b^*$,

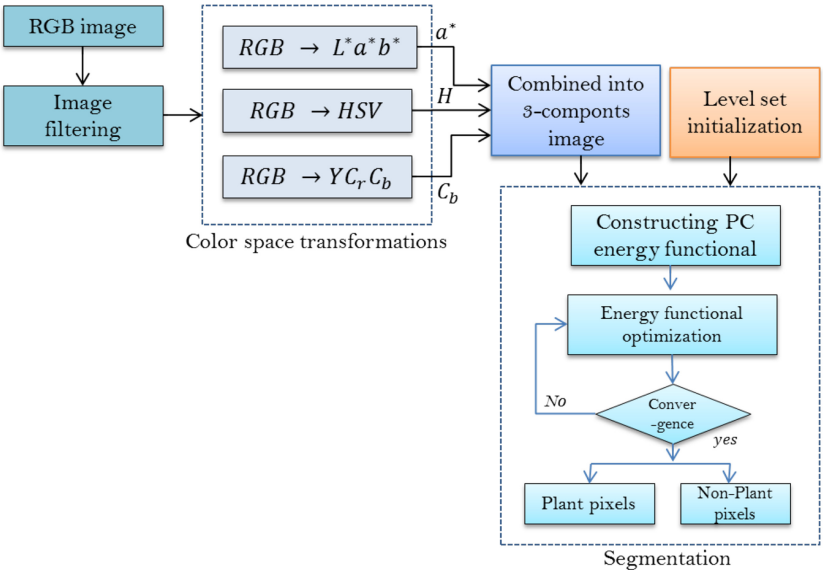

Fig. 1. Flowchart of proposed plant extraction

$L^*u^*v^*$, TSL, $I_1I_2I_3$ and XYZ. The best segmentation results are produced by the a^* channel in the $L^*a^*b^*$ color space. This later (a^*) was also used by Zhang et *al.*, in [6], to extract cotton leaves with disease under the field environment.

In all the previous cited works, the segmentation stage is done in a single-channel image. However, to broaden the benefit from the advantages of color spaces transformation, we propose to combine three components form the three best color spaces. Consequently, the image to be segmented is a multi-channel image constructed by a^*, H and C_b channels, obtained by color space transformations $L^*a^*b^*$ in Eq. (1), HSV in Eq. (2) and YC_rC_b in Eq. (3).

$$\begin{array}{l} L^* = \begin{cases} 116\,Y^{\frac{1}{3}} \text{ if } Y > k; \\ 903.3\,Y \text{ if } Y \leq k \end{cases} \text{ with k} = 0.008856 \\ a^* = 500(f(X) - f(Y)) \\ b^* = 200\,(f(Y) - f(Z)) \end{array} \quad , \quad f(t) = \begin{cases} f(t) = t^{\frac{1}{3}}, & \text{if } t > \text{k} \\ 7.787\ t + 0.1379 & \text{if } t \leq \text{k} \end{cases} \tag{1}$$

$$H = \begin{cases} \pi \quad \text{if } R = G = B \\ \arccos \dfrac{\frac{1}{2}\left[(R-G)+(R-B)\right]}{\sqrt{(R-G)^2+(R-B)(G-B)}} & \text{if} B \leqslant G \\ 2\pi - \arccos \dfrac{\frac{1}{2}\left[(R-G)+(R-B)\right]}{\sqrt{(R-G)^2+(R-B)(G-B)}} & \text{elsewhere} \end{cases}$$

$$S = \begin{cases} 0 & \text{if } R = G = B \\ 1 - \dfrac{3\min(R,G,B)}{R+G+B} & \text{elsewhere} \end{cases} \tag{2}$$

$$V = \frac{R + G + B}{3}$$

$$\begin{cases} Y = \ 0.299\,R \ + \ 0.587\,G \ + \ 0.114\,B \\ C_r = -0.169\,R \ - \ 0.331\,G \ + \ 0.500\,B \\ C_b = 0.500\,R \ - \ 0.419\,G \ - \ 0.081\,B \end{cases} \tag{3}$$

The obtained three-components image, noted by u_0, is free from luminance information and highlights well the foreground (plants) and attenuates the background (sol). This image is then used as the input to the segmentation algorithm.

2.2 Segmentation via Piecewise Constant PC Model

For the segmentation purpose, we use the famous energy-based model named Piecewise Constant Chan-Vese model in the biphase level set framework [14]. Chan-Vese bi-phase level set active contour is used for foreground/background separation. It is known by its good performance and robustness to noise. In the variational context, the PC model is defined as :

$$\begin{aligned} F(c^+, c^-, \Phi) = \ & \mu \int_\Omega \delta_\epsilon(\Phi(\mathbf{x}))|\nabla\Phi(\mathbf{x})|\,\mathbf{dx} + \int_\Omega \frac{1}{N}\sum_i^N \lambda_i^{in}\left|u_{0,i}(\mathbf{x}) - c_i^{in}\right|^2 \mathrm{H}_\epsilon(\Phi)\ \mathbf{dx} \\ & + \int_\Omega \frac{1}{N}\sum_i^N \lambda_i^{out}\left|u_{0,i}(\mathbf{x}) - c_i^{out}\right|^2 (1 - \mathrm{H}_\epsilon(\Phi)\ \mathbf{dx}, \qquad i = 1, \ldots N. \end{aligned} \tag{4}$$

where $u_{0,i}$ is the image to be segmented, $\Omega \in \mathbb{R}^2$ its domain definition and $\mathbf{x} = (x, y)$ represents the pixel coordinates. μ is scalar defining the length term weight and $\lambda_i^{in} > 0$ and $\lambda_i^{out} > 0$ weight coefficients for the error term inside and outside curve, respectively. H_ϵ is the regularized Heaviside function and δ_ϵ its derivative. $c^{in}(\Phi)$ and $c^{in}(\Phi)$ are the means inside and outside curve for each channels $(i, i = 1 \ldots 3)$, they are defined as follows:

$$c_i^{in}(\Phi) = \frac{\int_\Omega u_{0,i}\mathrm{H}_\epsilon(\Phi)\mathbf{dx}}{\int_\Omega \mathrm{H}_\epsilon(\Phi)\mathbf{dx}}, \ \ c_i^{out}(\Phi) = \frac{\int_\Omega u_{0,i}\,(1 - \mathrm{H}_\epsilon(\Phi))\,\mathbf{dx}}{\int_\Omega (1 - \mathrm{H}_\epsilon(\Phi))\,\mathbf{dx}} \tag{5}$$

In the present work, and to avoid the slow convergence of descent gradient optimization method, we use the sweep principal optimization algorithm. Therefor, two energies are evaluated for any movement of a pixel from inside to outside of curve as follows (see [15,16] for more details):

$$\Delta F_{12} = \frac{1}{N}\left[\sum_i^N \lambda_i \left(u_{0,i}(\mathbf{x}) - c_i^{out}\right)^2 \frac{n}{n+1} \ - \ \sum_i^N \lambda_i \left(u_{0,i}(\mathbf{x}) - c_i^{in}\right)^2 \frac{m}{m-1}\right] \tag{6}$$

$$\Delta F_{21} = \frac{1}{N}\left[\sum_i^N \lambda_i \left(u_{0,i}(\mathbf{x}) - c_i^{in}\right)^2 \frac{m}{m+1} \ - \ \sum_i^N \lambda_i \left(u_{0,i}(\mathbf{x}) - c_i^{out}\right)^2 \frac{n}{n-1}\right], \tag{7}$$

Finally, the segmented image is deducted as follows:

$$u_{seg} \ = \ \sum_{i=1}^{3} c_i^{in} \ \Big|_{\Phi>0} \ + \ \sum_{i=1}^{3} C_i^{out} \ \Big|_{\Phi<0} \tag{8}$$

3 Experimental Results

In all experiments, the level set is initialized automatically as a rectangle that takes the image size minus 10 pixels, this is done to avoid the interaction of the user. Furthermore, as the optimization is done via sweeping algorithm, we don't need to set the constants related to variational level set models [2]. The preprocessing stage is needed where image is noised, because we omit the length term in the optimized energy (Eq. (6) and (7)) as done in [17]. This step is done by a 3×3 Gaussian filter in the R, G, B components. Otherwise, the color space transformation stage is enough to decrease the noise effect.

3.1 Qualitative Evaluations

The proposed algorithm is tested on all *black nightshade* images of the open dataset downloaded from [18]. In total, *123* images of size $4256 \times 2832 \times 3$ acquired in uncontrolled outdoor light conditions and different growth stages.

The first experiment is devoted to represent each stage results of the proposed method on an arbitrary chosen image DSC_0645 displayed in Fig. 2a. The second row Fig. 2b shows the three components a^*, H and C_b obtained by color space transformations. The combination of those components gives a three-channel image (Fig. 2c). The zero level set is initialized on the image and the three level set (Fig. 2d). After seven iterations, the algorithm convergences correctly to the plants' contours. The segmentation outcomes is represented in Fig. 2e, where the converged level set is presented, the final zero level set contour is represented, with yellow line, on the input image to be more clear. In addition, the binary segmented image (on the middle of row). Finally, the extracted object is obtained by multiplying the final binary level set by the original RGB image.

The second experiment, shown in Fig. 3, is done on three black nightshade images acquired in cloudy, overcast and very sunny days. Thereby different lighting conditions: low, medium and strong lighting. This experiment highlights the ability of the proposed method to deal with light changing, where, in the three cases, the plants are correctly extracted from the soil.

Figure 4 shows comparison results between our method and the method proposed in [19] named improved principal component analysis (PCA)-based multichannel selection C-V model (PMCV). The principle of this method is the selection of three component from RGB and HSV color spaces by using PCA, then the Chan-Vese model was applied to segmentation of the wheat leaf lesions images. When the lighting is uniform (case of DSC_{0500} image), both models converge to the plant contours correctly. However for the image with strong lighting (DSC_{0628}) where the shadow is more strongly present, the PMPC model have tendency to an over segmentation, where several part of the sol strongly lighted is classed as the plants.



(a) RGB image DSC_0645

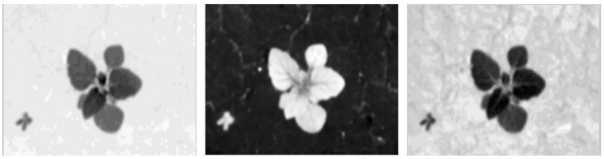

(b) From left to right : a^*, H and C_b channels

(c) u_0 image to be segmented

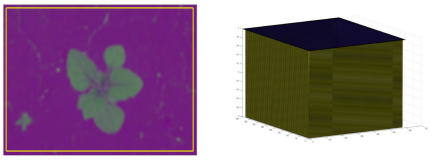

(d) Level set initialization



(e) Segmentation outcomes

Fig. 2. Outcomes of each stage of the proposed method. (a) input RGB original image, (b) The three components (a^*, H and C_b) obtained by color space transformationS. (c) The image after combination with initialized zero level set (yellow line) and corresponding level set function. (e) The algorithm outcomes: Final level set function, zero level set (yellow line) drawn on the original RGB image, segmented binary image u_{seg}, and extracted plant overlaid on the original image (Color figure online)

The last experiments are devoted to compare the proposed method performance against color index-based approaches, that are widely used in agricultural image segmentation. For that, two images from the dataset are chosen that present different light conditions and growing stages (DSC_0528 and DSC_0690). Furthermore, because there are a large color index-based formulations, we limit our comparisons to the ones classed as the best in the survey and evaluation done in [20], that are: Excess Green Index (ExG), Vegetative Index (VEG), Combined Indices 1 (COM1), Combined Indices 2 (COM2) and Excess Green minus Excess Red Index (ExGR), respectively. The segmentation

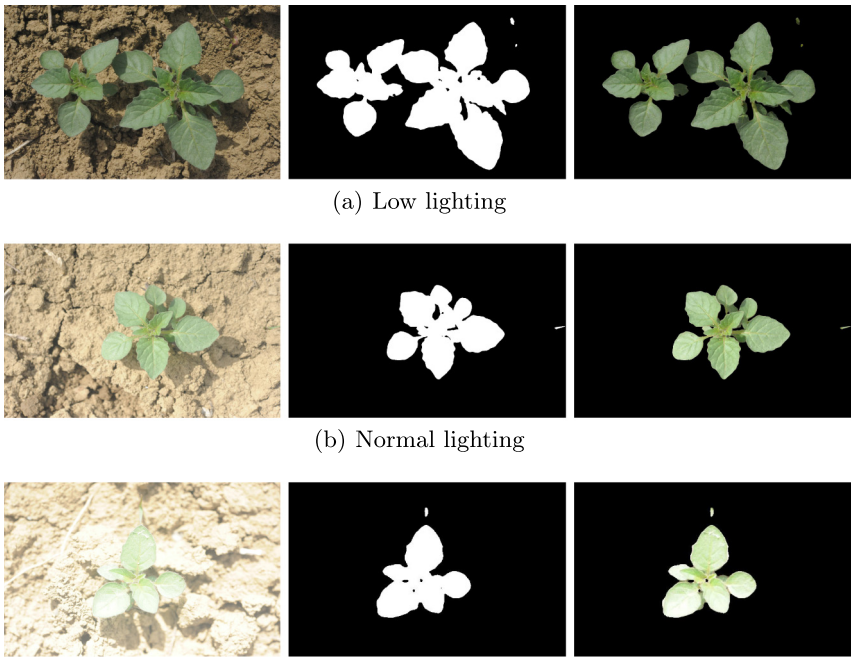

(a) Low lighting

(b) Normal lighting

(c) Strong lighting

Fig. 3. Examples of the proposed method performance on a set of images acquired in different natural light conditions. 1st row: clouded day. 2nd row: sunny day. 3th row: strongly sunny day

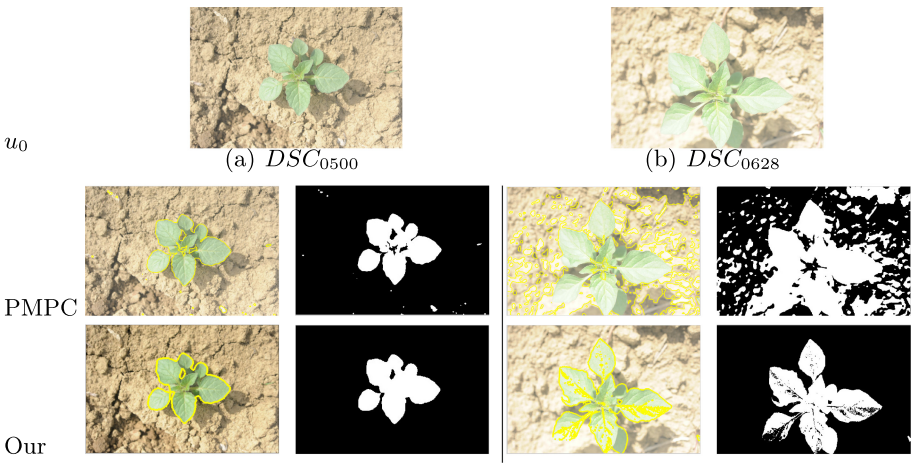

Fig. 4. Comparison of our method with the one based on HSV and RGB color spaces in [19].

is then applied using Otsu thresholding method. In Fig. 5, we display, for both images, the resulting image in each transformation and the segmentation results. COM1 and ExGR color index-based approaches completely fail to segment both images. However, ExG, VEG and COM2 have better performance. Compared to the proposed method, the segmentation is improved specially in terms of noise robustness and saturated pixels (due to very strong lighting).

3.2 Quantitative Evaluation of the Proposed Method Against Color Index-Based Approaches

The quantitative evaluation of the proposed method is made on three different public datasets that are:

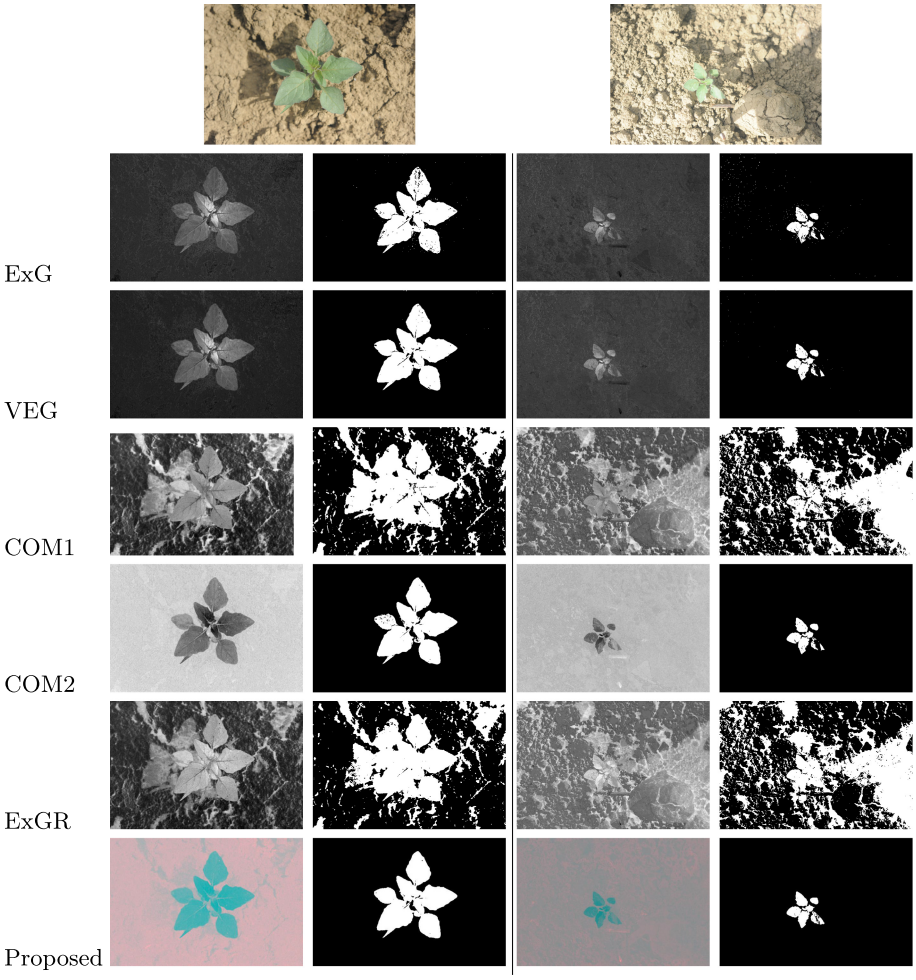

Fig. 5. Comparison of segmentation results obtained by Otsu-Color-Index approaches and the proposed one

- **CWFI (crop/weed field image) dataset** [21]: 60 RGB images (1296 × 966 pixels in resolution) acquired using ground vehicle, where the camera was shaded and artificially lit to avoid changing light conditions (controlled lighting).
- **Carrot-Weed dataset** [22]: it constitutes of 39 RGB images (1296 × 966) acquired using hand holding. They are taken under variable light conditions.
- **Wheat 2012 dataset** [23]: the acquisition system is done using camera mounted above the crop (2m). time-lapse images were taken and transmitted via 3G network. In this evaluation we use the folder named "wheat 2012" which contains 17 images (719 × 776) charactered by poor light conditions and complex background

The segmentation results are evaluated by using three different metrics Q_{seg}, $Jaccard$ and $Dice$, formulated as follows:

$$Q_{seg} = \frac{TP + TN}{FN + FP + TP + TN} \tag{9}$$

$$Dice = \frac{2TP}{2 * TP + FP + FN} \tag{10}$$

$$Jaccard = \frac{Dice}{2 - Dice} \tag{11}$$

The obtained results are summarized by the mean accuracy rate of each metric and each dataset (see Fig. 6). The comparison is done against the Excess

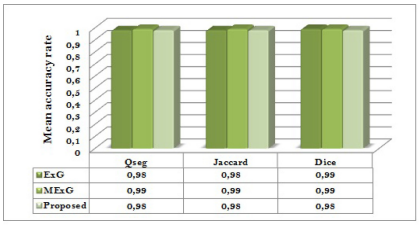

(a) CWFI dataset

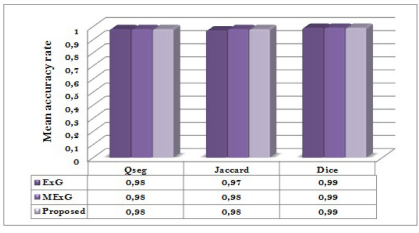

(b) Carrot-Weed dataset

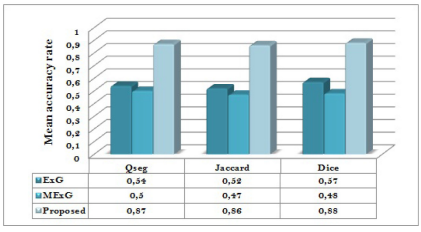

(c) Wheat 2012 dataset

Fig. 6. Quantitative evaluation of the proposed method against ExG and MExG for three different datasets using three evaluation metrics

Green Index (ExG) and the Modified Excess Green Index (MExG). This evaluation revels that the three methods give similar performance on the two first datasets (CWFI and Carrot-Weed datasets). However, the proposed method improves considerably the performance on the *wheat 2012* dataset.

4 Conclusion

This paper proposed a method to segment plants images acquired in uncontrolled outdoor lighting. Thereby those RGB images are noised, shadowed, saturated, and uneven lighting. Our method is based on a multichannel-Fast- Chan-Vese segmentation. It exploits chroma information by using three color space transformations, then a^*, H and C_b components are selected to construct the image to be segmented. Segmentation step is assured by the generalized Chan-Vese model implemented with bi-phase level set. Furthermore, the optimization of energy functional is done via sweep algorithm to ensure a fast convergence.

The obtained results allow us to see the good performance of our method in very challenging situations. Compared to color index-based approaches and PMPC model, our method improves the segmentation.

References

1. Hernández-Hernández, J.L., et al.: A new portable application for automatic segmentation of plants in agriculture. Agric. Water Manage. **183**, 146–157 (2017)
2. Boutiche, Y., Abdessalem, A., Ramou, N., Chetih, N.: Fast generalized Chan-Vese model for plant/soil segmentation to estimate percentage of ground cover in agricultural images. In: 2019 IEEE International Symposium on Signal Processing and Information Technology (ISSPIT), December 2019, pp. 1–5 (2019)
3. Guo, W., Rage, U.K., Ninomiy, S.: Illumination invariant segmentation of vegetation for time series wheat images based on decision tree model. Comput. Electron. Agric. **96**, 58–66 (2013)
4. Wang, Z., Wang, K., Yang, F., Pan, S., Han, Y.: Image segmentation of overlapping leaves based on Chan-Vese model and Sobel operator. Inf. Process. Agric. **5**, 1–10 (2018)
5. Singh, V., Misra, A.K.: Detection of plant leaf diseases using image segmentation and soft computing techniques. Inf. Process. Agric. **4**, 41–49 (2017)
6. Zhang, J., Kong, F., Wu, J., Han, S., Zhai, Z.: Automatic image segmentation method for cotton leaves with disease under natural environment. J. Integr. Agric. **17**, 180–1814 (2018)
7. Maldonado, W., Barbosa, J.C.: Automatic green fruit counting in orange trees using digital images. Comput. Electron. Agric. **127**, 572–581 (2016)
8. Busin, L., Vandenbroucke, N., Macaire, L.: Color spaces and image segmentation. Adv. Imaging Electron Phys. **151**, 65–168 (2008)
9. Jurio, A., Pagola, M., Galar, M., Lopez-Molina, C., Paternain, D.: A comparison study of different color spaces in clustering based image segmentation. In: Hüllermeier, E., Kruse, R., Hoffmann, F. (eds.) IPMU 2010. CCIS, vol. 81, pp. 532–541. Springer, Heidelberg (2010). https://doi.org/10.1007/978-3-642-14058-7_55

10. García-Mateos, G., Hernández, J.L., Escarabajal-Henarejos, D., Jaén-Terrones, S., Molina-Martínez, J.M.: Study and comparison of color models for automatic image analysis in irrigation management applications. Agric. Water Manage. **151**, 158–166 (2015)
11. Wang, A., Zhang, W., Wei, X.: A review on weed detection using ground-based machine vision and image processing techniques. Comput. Electron. Agric. **158**, 226–240 (2019)
12. Macaire, L., Postaire, J.G.: Color systems coding for color image. In: Proceedings of International Conference on Color in Graphics and Image Processing (CGIP 2000), Saint-Etienne, France, October, pp. 180–185 (2000)
13. Farid, G.-L., Jair, C., Asdrubal, L.-C., Lisbeth, R.: Segmentation of images by color features: a survey. Neurocomputing **292**, 1–27 (2018). https://doi.org/10.1016/j.neucom.2018.01.091
14. Chan, T.F., Sandberg, B.Y., Vese, L.A.: Active contours without edges for vector-valued images. J. Vis. Commun. Image Representation **11**, 130–141 (2000)
15. Boutiche, Y., Abdesselam, A.: Fast algorithm for hybrid region-based active contours optimisation. IET Image Process. **11**, 200–209 (2017). https://doi.org/10.1049/iet-ipr.2016.0648
16. Song, B., Chan, T.: A fast algorithm for level set based optimization. CAM-UCLA **2**(68), pp. 2–68 (2002)
17. He, L., Osher, S.: A fast multiphase level set algorithm for solving the Chan-Vese model. In: Proceedings in Applied Mathematics and Mechanics, vol. 7, pp. 1041911–1041912 (2007)
18. Espejo-Garcia, B., Mylonas, N., Athanasakos, L., Fountas, S., Vasilakoglou, I.: Towards weeds identification assistance through transfer learning. Comput. Electron. Agric. **171**, 105306 (2020)
19. Qiu-xia, H., Tian, J., He, D.: Wheat leaf lesion color image segmentation with improved multichannel selection based on the Chan-Vese model. Comput. Electron. Agric. **135**, 260–268 (2017)
20. Hamuda, E., Glavin, M., Jones, E.: A survey of image processing techniques for plant extraction and segmentation in the field. Comput. Electron. Agric. **125**, 184–199 (2016)
21. Haug, S., Ostermann, J.: A crop/weed field image dataset for the evaluation of computer vision based precision agriculture tasks. In: Agapito, L., Bronstein, M.M., Rother, C. (eds.) ECCV 2014. LNCS, vol. 8928, pp. 105–116. Springer, Cham (2015). https://doi.org/10.1007/978-3-319-16220-1_8
22. Lameski, P., Zdravevski, E., Trajkovik, V., Kulakov, A.: Weed detection dataset with RGB images taken under variable light conditions. In: Trajanov, D., Bakeva, V. (eds.) ICT Innovations 2017. CCIS, vol. 778, pp. 112–119. Springer, Cham (2017). https://doi.org/10.1007/978-3-319-67597-8_11
23. Guo, W., Zheng, B., Duan, T., Fukatsu, T., Chapman, S., Ninomiya, S.: EasyPCC: benchmark datasets and tools for high-throughput measurement of the plant canopy coverage ratio under field conditions. Sensors **17**, 798 (2017). https://doi.org/10.3390/s17040798